Special Collection

Microscopic Reactivity of Phenylferrate Ions toward Organyl Halides

Stefan Lülf+,[a] Luxuan Guo+,[b] Tobias Parchomyk,[a] Jeremy N. Harvey,*[b] and Konrad Koszinowski*[a, c]

In memory of Ulf Diederichsen.

Abstract: Despite its practical importance, organoiron chemistry remains poorly understood due to its mechanistic complexity. Here, we focus on the oxidative addition of organyl halides to phenylferrate anions in the gas phase. By mass-selecting individual phenylferrate anions, we can determine the effect of the oxidation state, the ligation, and the nuclearity of the iron complex on its reactions with a series of organyl halides RX. We find that $Ph_2Fe(I)^-$ and other low-valent ferrates are more reactive than $Ph_3Fe(II)^-$; $Ph_4Fe(III)^-$ is inert. The coordination of a PPh_3 ligand or the presence of a second iron center lower the reactivity. Besides direct cross-coupling reactions resulting in the formation of RPh, we also observe the abstraction of halogen atoms. This reaction channel shows the readiness of organoiron species to undergo radical-type processes. Complementary DFT calculations afford further insight and rationalize the high reactivity of the $Ph_2Fe(I)^-$ complex by the exothermicity of the oxidative addition and the low barriers associated with this reaction step. At the same time, they point to the importance of changes of the spin state in the reactions of $Ph_3Fe(II)^-$.

Introduction

Situated in the center of the periodic table well within the 3d block, iron can adopt a wide range of different oxidation and coordination states. For this reason, this metal shows a rich and complex chemistry, which gives rise to numerous catalytic applications. This also holds true for *organo*iron chemistry. Among the different catalytic processes of this type, iron-mediated Kumada-type cross-coupling reactions between organyl halides and Grignard reagents, Equation (1), are particularly promising.[1]

$$RX + R'MgX \xrightarrow{[Fe]} RR' + MgX_2 \qquad (1)$$

The full potential of these transformations has not been realized yet because of a lack of mechanistic understanding. Without this understanding, it is impossible to optimize these reactions in a systematic and rational manner. The mechanistic elucidation of iron-catalyzed cross-coupling reactions is challenging due to the relatively low stability of organoiron intermediates and their tendency to undergo fast equilibration reactions in solution, which result in complex mixtures of different iron species.[2] For this reason, not even the oxidation state of the active catalyst is known with certainty, with suggestions ranging from $-II$ to $+II$.[3]

In the present study, we confine ourselves to the analysis of the elementary step of the oxidative addition and take a rigorously reductionist approach by probing the intrinsic microscopic reactivity of phenylferrate anions toward organyl halides in the gas phase.[4] We focus on anionic species not only for facilitating the gas-phase experiments, but also due to the supposed role of organoferrates R'_mFe^- as catalytic intermediates in cross-coupling reactions.[4] As we have shown previously, gaseous phenylferrates $Ph_mFe_n(PPh_3)_x^-$ can be prepared in different oxidation, aggregation and ligation states and are therefore particularly well-suited as model systems.[5] By mass-selecting the ions in the gas phase, we can exclude redox-equilibration processes, which occur in solution and contribute to the notorious complexity of the reaction mixtures. Moreover, the absence of solvent molecules, counter-ions, and other

[a] S. Lülf,+ Dr. T. Parchomyk, Prof. Dr. K. Koszinowski
Institut für Organische und Biomolekulare Chemie
Universität Göttingen
Tammannstr. 2, 37077 Göttingen (Germany)
E-mail: konrad.koszinowski@chemie.uni-goettingen.de
Homepage: https://www.uni-goettingen.de/de/321433.html

[b] L. Guo,+ Prof. Dr. J. N. Harvey
Department of Chemistry
KU Leuven
Celestijnenlaan 200F, B-3001 Leuven (Belgium)
E-mail: jeremy.harvey@kuleuven.be
Homepage: https://chem.kuleuven.be/en/research/qcpc/tccx

[c] Prof. Dr. K. Koszinowski
Wöhler Research Institute for Sustainable Chemistry
Universität Göttingen
Tammannstr. 2, 37077 Göttingen (Germany)

[+] These authors contributed equally to this work.

📖 Supporting information for this article is available on the WWW under https://doi.org/10.1002/chem.202202030

Special Collection This article belongs to a Joint Special Collection dedicated to Ulf Diederichsen.

Chem. Eur. J. **2022**, *28*, e202202030 (1 of 8)

© 2022 The Authors. Chemistry - A European Journal published by Wiley-VCH GmbH

potential reactants in the present experiments prevents unwanted consecutive reactions. Thus, we achieve full control over the systems under scrutiny.[7–9] Furthermore, the gas-phase environment is ideally suited for comparing the experimental results with the predictions of quantum chemical calculations. These calculations can afford structural and energetic data not directly deducible from the experiments. Together, experiment and theory thereby promise to give detailed insight into the fundamental reactivity of isolated organoiron species. Although this insight does not directly apply to the real catalytic system in solution, we see our study as the first step in a bottom-up strategy. By including the effect of individual solvent molecules and counter-ions, the present-gas phase model can be gradually refined and extended to approach the solution-phase reaction eventually.

Results and Discussion

Preparation of gaseous phenylferrate complexes

Transmetalation of $Fe(acac)_3$ with an excess of PhMgCl in the presence of PPh_3 followed by negative-ion mode electrospray ionization (ESI) produced a mixture of gaseous $[Ph_3Fe]^-$, $[Ph_4Fe]^-$, $[Ph_2Fe(PPh_3)]^-$, and $[Ph_3Fe_2(PPh_3)]^-$ (Figures S1 and S2). Gas-phase fragmentation of the mass-selected ions afforded the additional ions $[Ph_2Fe]^-$, $[Fe,P,Ph_3]^-$, and $[Ph,Fe_2,P,Ph_3]^-$ (see Scheme S1 in the Supporting Information for details). The iron centers in the phosphine-free complexes $[Ph_mFe]^-$ have oxidation states between $+I$ and $+III$. For their phosphine-containing counterparts, the situation is more complicated because it is not immediately clear whether the phosphine ligand in these species remains intact or whether it has undergone a metal insertion, such as an activation of a C–P bond[10] or an *ortho*-metalation.[11] To address this problem, we performed control experiments, in which both PPh_3 and $PTol_3$ were added simultaneously. The resulting ESI mass spectra showed phenylferrates with either one of the two phosphines, but did not give any evidence of scrambling of the Ph and Tol groups (Figures S3–S4). This finding strongly suggests that the complexes $[Ph_2Fe(PPh_3)]^-$ and $[Ph_3Fe_2(PPh_3)]^-$ indeed contain intact phosphine ligands. Accordingly, we can assign average oxidation states of $+I$ to the iron centers in these species. In contrast, we cannot rule out that the complexes $[Fe,P,Ph_3]^-$ and $[Ph,Fe_2,P,Ph_3]^-$ have undergone iron insertion into C–P bonds in
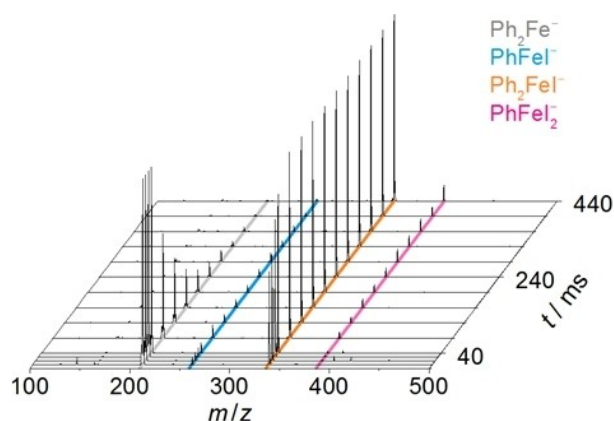
Figure 1. Mass spectra of mass-selected $[Ph_2Fe]^-$ (m/z 210) and its product ions formed upon reaction with vinyl iodide after different reaction times t.

the course of the gas-phase fragmentation reactions required for their preparation. Consequently, the oxidation states of these species must remain open.

Gas-phase reactions of phenylferrate complexes with organyl halides

To characterize the microscopic reactivity of the phenyferrates, we subjected them to collisions with a series of organyl halides RX. $[Ph_2Fe^I]^-$ reacted with a wide range of organyl iodides and bromides (Figures 1 and S5–S23), but not with ^iPrCl (Table 1). The main reaction channel corresponded to a halogen transfer, Equation (2). This type of reactivity highlights the well-known propensity of iron to undergo radical reactions.[1a,6b]

$$[Ph_2Fe]^- + RX \rightarrow [Ph_2FeX]^- + R^\bullet \tag{2}$$

For the reaction of $[Ph_2Fe^I]^-$ with PhI, we also performed a control experiment, in which we replaced PhI by its C_6D_5I isotopologue (Figure S7). Here, we only observed the loss of the $C_6D_5^\bullet$ radical, Equation (3a), but not that of $Ph^\bullet$, Equation (3b). This finding excludes a complete equilibration of the Ph and C_6D_5 groups.

$$[Ph_2Fe]^- + C_6D_5I \rightarrow [Ph_2FeI]^- + C_6D_5^\bullet \tag{3a}$$

Table 1. Gas-phase reactivity of mass-selected phenylferrate anions toward organyl halides ($+$: $k \geq 10^{-12}\,cm^3\,s^{-1}$, $-$: $k < 10^{-12}\,cm^3\,s^{-1}$).

$Ph_mFe_n(PPh_3)_x^-$	oxidation state	C_2H_3I[a]	PhI	MeI	EtI	^iPrCl	^iPrBr	^iPrI	^tBuI	C_3H_5Br[b]	C_3H_5I[b]
Ph_2Fe^-	$+I$	$+$[c,d]	$+$[c,d]	$+$[c,d]	$+$[c,d]	$-$	$+$[c]	$+$[c]	$+$[c,d]	$+$[c,d]	$+$[c,d]
Ph_3Fe^-	$+II$	$-$	$-$	$-$	$-$	$-$	$-$	$-$	$-$	$+$[d]	$-$
Ph_4Fe^-	$+III$	$-$	$-$	$-$	$-$	$-$	$-$	$-$	$-$	$-$	$-$
$Ph_2Fe(PPh_3)^-$	$+I$	$-$	$-$	$-$	$-$	$-$	$-$	$-$	$-$	$-$	$-$
$Ph_3Fe_2(PPh_3)^-$	$+I$	$-$	$-$	$-$	$-$	$-$	$-$	$-$	$-$	$-$	$-$
$[Ph,Fe_2,P,Ph_3]^-$	$0/+I$	$+$[c,d]	$+$[c,d]	$+$[c]	$+$[c]	$-$	$-$	$+$[c]	$+$[c]	$+$[c,d]	$+$[c,d]
$[Fe,P,Ph_3]^-$	$-I/+I$	$+$[c]	$-$	$+$[d,e]	$+$[c]	$-$	$-$	$+$[c]	$+$[c]	$+$[d,e]	$+$[d,e]

[a] $C_2H_3 =$ vinyl. [b] $C_3H_5 =$ allyl. [c] Halogen transfer, Equation (2). [d] Direct cross-coupling, Equation (4).

Chemistry–A European Journal

Research Article
doi.org/10.1002/chem.202202030

Chemistry
Europe
European Chemical
Societies Publishing

$$[Ph_2Fe]^- + C_6D_5I \nrightarrow [Ph(C_6D_5)FeI]^- + Ph^\bullet \tag{3b}$$

In several cases, we also observed a second reaction channel, in which the halogen transfer to $[Ph_2Fe]^-$ was accompanied by the loss of a phenyl group from the ferrate, Equation (4).

$$[Ph_2Fe]^- + RX \rightarrow [PhFeX]^- + [R,Ph] \tag{4}$$

The identity of the neutral formed in this reaction is a priori not obvious. It could either correspond to the cross-coupling product R–Ph or to separate $R^\bullet$ and $Ph^\bullet$ radicals, with the latter being released from the energized product of the halogen transfer, Equation (2). However, the second possibility appears less probable for the reactions starting from $[Ph_2Fe]^-$ and furnishing $[Ph_2FeX]^-$ as primary product because the closely related $[Ph_3Fe]^-$ is known to eliminate benzene instead of a phenyl radical upon the provision of energy;[6a] this behavior again reflects the rather low stability of $Ph^\bullet$. To obtain more direct evidence, we subjected the mass-selected Ph_2FeI^- product ion to a fragmentation experiment, which mainly afforded I^-, but hardly any $[PhFeI]^-$ (Figure S24). This result excludes the possibility that the $[PhFeX]^-$ ions originate from a consecutive decomposition of $[Ph_2FeX]^-$ and, thus, implies that the neutral formed in this reaction corresponds to the cross-coupling product RPh. Furthermore, the aforementioned labeling experiment produced not only $[PhFeI]^-$ as product ion, Equation (5a), but $[(C_6D_5)FeI]^-$ as well, Equation (5b). The apparent equilibration of the labeled and unlabeled phenyl groups proves the involvement of the $[Ph_2(C_6D_5)Fe^{III}I]^-$ adduct for this reaction channel. The $[PhFeX]^-$ product ions also underwent consecutive halogen-transfer reactions. Analogous consecutive reactions did not occur for their $[Ph_2FeX]^-$ counterparts.

$$[Ph_2Fe]^- + C_6D_5I \rightarrow [PhFeI]^- + C_6D_5Ph \tag{5a}$$

$$[Ph_2Fe]^- + C_6D_5I \rightarrow [(C_6D_5)FeI]^- + Ph_2 \tag{5b}$$
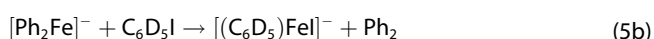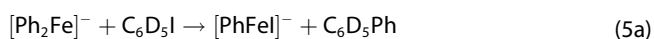
For the reaction of $[Ph_2Fe]^-$ with MeI, we observed not only the iodine-transfer and direct cross-coupling channels, but the formation of significant quantities of $[MeFeI]^-$, Equation (6), as well (Figure S8). This product then apparently underwent a consecutive iodine transfer to afford $[MeFeI_2]^-$. The formation of $[MeFeI]^-$ can be understood as an oxidative addition of MeI accompanied by the reductive elimination of Ph_2. Most likely, the latter is driven by the energy released from the oxidative addition. Interestingly, an analogous reaction did not occur for any of the other substrates (except for C_6D_5I, see above). Possibly, the special behavior encountered for the reaction of MeI originated from the small size of this substrate. The correspondingly smaller number of degrees of freedom for this system may imply that the excess energy resulting from the initial oxidative addition can more easily accumulate in the reactive mode and, thus, give rise to the reductive elimination of Ph_2.

$$[Ph_2Fe]^- + MeI \rightarrow [MeFeI]^- + Ph_2 \tag{6}$$
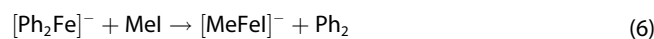
Next, we examined the reactivity of $[Ph_3Fe^{II}]^-$ and $[Ph_4Fe^{III}]^-$ toward organyl halides. $[Ph_3Fe^{II}]^-$ reacted only with allyl bromide to afford $[Ph_2FeX]^-$ as the ionic product (Table 1 and Figure S25). Again, it is not immediately clear whether this reaction furnished the cross-coupling product C_3H_5Ph or separate $C_3H_5^\bullet$ and $Ph^\bullet$ radicals. Obviously, the former alternative would be energetically much more favorable and can also be expected to involve lower barriers. As the negligible reactivity of $[Ph_3Fe^{II}]^-$ toward all other probed substrates suggests, the reactions of this ion with organyl halides are energetically much more demanding than those of its $[Ph_2Fe^I]^-$ counterpart. For this reason, we consider it more likely that the observed reaction forms the cross-coupling product RPh, Equation (7) with R = allyl, rather than furnishing separate radicals. Our quantum chemical calculations fully supported this assumption (see below). Unlike $[Ph_3Fe^{II}]^-$, $[Ph_4Fe^{III}]^-$ did not react with any of the substrates included (Table 1). These findings show that the tendency to undergo oxidative additions decreases in the order $k(Fe^I) > k(Fe^{II}) > k(Fe^{III})$. This order is also consistent with the lack of reactivity of the $[Ph_2FeX]^-$ primary products (see above).

$$[Ph_3Fe]^- + RX \rightarrow [Ph_2FeX]^- + RPh \tag{7}$$

The coordination of PPh_3 to mono- and dinuclear phenylferrates(I) shuts off their reactivity (Table 1). In contrast, the phosphine-containing low-valent ferrates $[Ph,Fe_2,P,Ph_3]^-$ and $[Fe,P,Ph_3]^-$ also reacted with most of the probed organyl halides (Figures S26–S40 and Table 1). Although the connectivity of these complexes remains unknown (see above), they most likely contain coordinatively unsaturated iron centers, which explains their high reactivity.

Rate constants of the reactions of $[Ph_2Fe]^-$

To obtain more detailed mechanistic insight, we analyzed the time dependence of the $[Ph_2Fe]^-$/RX reactions in a quantitative manner. The presence of the neutral substrate RX in a large excess relative to $[Ph_2Fe]^-$ ensured pseudo-first order conditions, as was directly evident from the exponential decrease of the normalized signal intensity of the reactant $[Ph_2Fe]^-$ ions (Figures 2 and S5–S23). Fitting of the measured signal intensities afforded sets of pseudo-first order rate constants, from which the bimolecular rate constants of the primary and consecutive reactions could be easily calculated on the basis of the known partial pressures $p(RX)$ in the ion trap (for the used kinetic model, see Scheme S2). A comparison of the determined rate constants and the corresponding reaction efficiencies showed a marked dependence on the nature of the substrate RX (Table 2). The measured rate constants increase in the order $k(RCl) < k(RBr) < k(RI)$, reflecting decreasing R–X bond-dissociation energies. Among the considered organyl iodides RI, allyl iodide underwent the fastest iodine transfer and phenyl iodide

Chemistry–A European Journal

Research Article
doi.org/10.1002/chem.202202030

Chemistry Europe
European Chemical
Societies Publishing
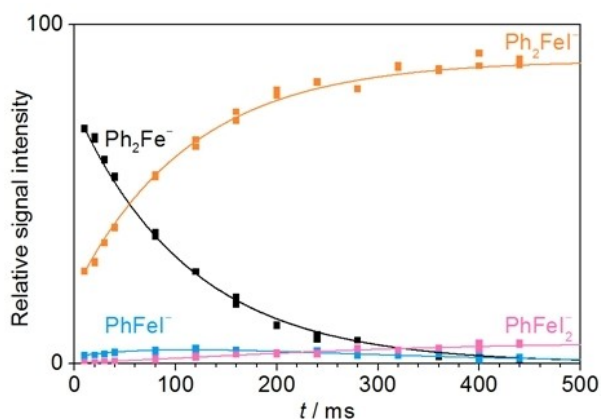
Figure 2. Time dependence of the normalized signal intensities of [Ph$_2$Fe]$^-$ and its product ions formed upon reaction with vinyl iodide (symbols) together with fit (lines).

the slowest. However, the efficiencies of these reactions differ only by a factor of 14 whereas the radical stabilization energies of the C$_3$H$_5^{\bullet}$ and Ph$^{\bullet}$ radicals span a range of >100 kJ mol^{-1}.[12] This comparison shows that the stability of the R$^{\bullet}$ radical formed during the reaction, Equation (2), is not the major factor controlling the facility of the halogen transfer. With respect to the direct cross-coupling reaction, we observed the highest efficiency for MeI.

Reactivity of Ph$_2$Fe$^-$ toward tetrahydrofuran

The high reactivity of [Ph$_2$Fe]$^-$ toward organyl bromides and iodides observed in the present gas-phase experiments suggests that this species, as well as other low-valent organoferrates, may also react with these substrates in solution. If [Ph$_2$Fe]$^-$ or related low-valent and coordinatively unsaturated complexes really do correspond to the catalytically active species in iron-mediated cross-coupling reactions, it is essential that they react with the RX substrates in a selective manner, but not with any other components present in the reaction mixture.

In particular, they must not react with the solvent. To exclude this possibility, we also subjected mass-selected [Ph$_2$Fe]$^-$ to collisions with THF, a solvent typically used in iron-catalyzed cross-coupling. The absence of any significant reaction apart from oxidation reactions by residual traces of O$_2$ (ϕ(THF) $<$ 4×10^{-3} cm^3 s^{-1}) demonstrates that [Ph$_2$Fe]$^-$ and related low-valent species do not react in an unselective manner (Figure S41). This notion is fully consistent with the previously reported formation of the Fe(I) ions [Bu$_2$Fe]$^-$ and [Ph$_2$Fe(Ph$_2$)]$^-$ in solutions of THF.[5e,6b]

Potential energy surfaces of [Ph$_2$Fe]$^-$/RX systems

In order to understand the difference in reactivity observed experimentally between [Ph$_2$Fe^I]$^-$ and [Ph$_3$Fe^{II}]$^-$, DFT calculations were conducted with these ions and different organyl halide substrates (for key structures, see Figures S42–S46). We first consider the [Ph$_2$Fe]$^-$/C$_2$H$_3$I system. [Ph$_2$Fe^I]$^-$ is predicted to have a quartet ground state at the UB3LYP-D3BJ/def2TZVP// def2SVP level of theory, and this assignment was supported by CCSD(T)-F12 benchmark results for the related [Me$_2$Fe]$^-$ system (see Supporting Information for details, Table S2). The doublet and sextet states lie much higher in energy by 150 and 93 kJ mol^{-1}, respectively, and indeed the quartet surface remains lowest throughout the reaction, although the energy gap is smaller for some intermediates (Figure S47). Reactants Ph$_2$Fe$^-$ and C$_2$H$_3$I can form a π complex lying 140 kJ mol^{-1} below the reactants, which can undergo facile oxidative addition through a transition state for C–I bond activation with an energy barrier of 22 kJ mol^{-1} to yield an Fe(III) species [Ph$_2$FeI(C$_2$H$_3$)]$^-$ (Figures 3 and S42). An alternative transition state (TS) for iodine-atom abstraction in which the Fe center does not interact with the vinyl group was found to be much higher in energy (−15 versus −118 kJ mol^{-1}, see Figure 3).

The oxidative adduct [Ph$_2$FeI(C$_2$H$_3$)]$^-$ can undergo reductive elimination to form the cross-coupling products styrene and [PhFeI]$^-$, or Fe-vinyl bond homolysis to yield halogen-transfer products [Ph$_2$FeI]$^-$ and a vinyl radical. Depending on the detailed reaction dynamics, the latter products may also be formed directly from the C–I bond activation TS without visiting

Table 2. Bimolecular rate constants k (10^{-11} cm^3 s^{-1}) as well as efficiencies ϕ of the halogen-transfer, Equation (2), and direct cross-coupling reaction, Equation (4), respectively, between [Ph$_2$Fe]$^-$ and organyl halides RX.

RX	Halogen transfer		Direct cross-coupling	
	$k(2)$	$\phi(2)$	$k(4)$	$\phi(4)$
^{i}PrCl	<0.02	$<2 \times 10^{-4}$	<0.02	$<2 \times 10^{-4}$
^{i}PrBr	3.2 ± 1.0	0.02 ± 0.01	0.04 ± 0.2	$3 \pm 15 \times 10^{-4}$
C$_3$H$_5$Br[a]	94 ± 13	0.72 ± 0.10	0.6 ± 0.2	$5 \pm 2 \times 10^{-3}$
MeI	30 ± 10	0.27 ± 0.09	33 ± 11	0.31 ± 0.10
EtI	51 ± 17	0.40 ± 0.13	8.4 ± 2.8	0.07 ± 0.02
^{i}PrI	45 ± 15	0.35 ± 0.12	0.04 ± 0.1	$3 \pm 8 \times 10^{-4}$
^{t}BuI	47 ± 16	0.34 ± 0.12	2.6 ± 0.8	0.02 ± 0.01
C$_3$H$_5$I[a]	124 ± 41	1.00 ± 0.33	17 ± 6	0.14 ± 0.05
C$_2$H$_3$I[b]	39 ± 13	0.38 ± 0.13	3.7 ± 1.2	0.04 ± 0.01
PhI	8.0 ± 2.6	0.07 ± 0.02	0.8 ± 0.7	0.01 ± 0.01

[a] C$_3$H$_5$ = allyl. [b] C$_2$H$_3$ = vinyl.

Chemistry–A European Journal

Research Article
doi.org/10.1002/chem.202202030

Chemistry
Europe
European Chemical
Societies Publishing
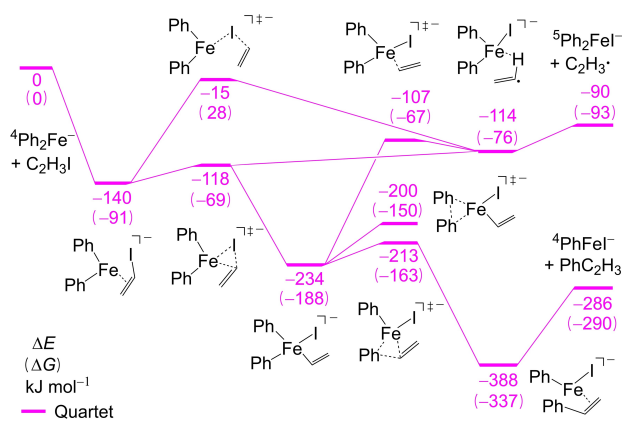
Figure 3. Potential and free energy surface for the [Ph$_2$Fe]$^-$/C$_2$H$_3$I system (for $T = 298.15$ K).

the well corresponding to the oxidative adduct intermediate. Both reactions are predicted to be overall very exothermic, consistent with the observation of both types of product. Like the reactant, the Fe(I) cross-coupling product [PhFeI]$^-$ has a quartet ground state, whereas the Fe(II) halogen-transfer product [Ph$_2$FeI]$^-$ has a quintet ground state (which, together with the concomitantly formed vinyl radical means that the product correlates with a quartet and sextet potential energy surface).

Prediction of the branching ratio is difficult as it depends on competition between passage through the 'tight' reductive elimination saddle-point and the more loosely structured variational TS for Fe-vinyl homolysis, and also on the possibility for direct vinyl loss without visiting the oxidative adduct well. The observation that only C$_6$D$_5$$^\bullet$ radicals are released in reactions of Ph$_2$Fe$^-$ with the rather similar C$_6$D$_5$I suggests that such direct halogen transfer can compete with routes leading through the oxidative adduct, but very demanding dynamics simulations going beyond the scope of this work would be needed to assess such routes. Based on its calculated potential energy, the intermediate [Ph$_2$FeI(C$_2$H$_3$)]$^-$ will be formed with over 230 kJ mol^{-1} of vibrational energy. In the highly diluted gas phase, this energy will not dissipate into the environment, but remain in the intermediate and can drive either homolysis or reductive elimination. Both of these dissociation channels lie far below the reactants and, thus, are energetically well feasible. As more energy will initially be present in the Fe-vinyl mode than in for example the Fe-phenyl modes and as the very high internal energies can be expected to result in extremely fast dissociations, dynamical effects may also play an important role in defining the selectivity.[13] The alternative homolytic steps leading to Fe–Ph or Fe–I bond-breaking in [Ph$_2$FeI(C$_2$H$_3$)]$^-$ are predicted to require more energy than Fe-vinyl bond breaking by 43 and 117 kJ mol^{-1}, respectively (Table S3), consistent with their non-occurrence in the experiments. In Figure 3, we show the TS for coupling of vinyl and phenyl groups to yield reductive elimination of Ph-CH=CH$_2$. In principle, reductive elimination by the competing homo-coupling channel is also possible. We have located this TS in the quartet state, where it

is found to lie higher in energy than that for cross-coupling by 13 kJ mol^{-1} (Figure 3), consistent with the non-occurrence of this homo-coupling process in the experiments.[14]

In the case of [Ph$_2$Fe]$^-$/C$_3$H$_5$Br, the reactant [Ph$_2$Fe]$^-$ also forms a π complex with allyl bromide lying 115 kJ mol^{-1} in energy below the reactants (Figures S43 and S48). Attempts to locate a saddle-point for C–Br bond activation were unsuccessful, with calculations involving scanning the energy upon increasing or decreasing the C–Br distance indicating an almost barrierless energy profile (see Supporting Information for details, Figures S49 and S50), so C–Br activation should be very fast, consistent with the high observed reaction efficiency. The computations again do not readily lead to a predicted branching behavior between cross-coupling and halogen abstraction.

For the [Ph$_2$Fe]$^-$/^{i}PrBr system, the reactant complex does not involve stabilizing π-complex interactions and is less strongly bound, by only 48 kJ mol^{-1} (Figures S44 and S51). The TS for bromine abstraction lies only 16 kJ mol^{-1} below the entrance channel, consistent with the lower reaction efficiency of 0.02.

For the reaction with [Ph$_2$FePPh$_3$]$^-$, computation shows a similar strength of binding of vinyl iodide in the π complex (−137 kJ mol^{-1}) to the phosphine-free case (−140 kJ mol^{-1}), with a low energy barrier of 28 kJ mol^{-1} for C–I bond activation (Figure S52). However, the structure of the Ph$_2$FePPh$_3$ moiety in the π complex is somewhat distorted compared to the free ion, due to steric crowding around the iron center, suggesting that this complex may not be readily formed. A more weakly bound σ complex with less distortion at the iron center can be formed, but the TS for its rearrangement to the π complex lies 7 kJ mol^{-1} higher in free energy than separated reactants, suggesting that steric effects may prevent formation of the π complex and thereby account for the lack of reactivity for this phosphine-coordinated ion.

Potential energy surfaces of [Ph$_3$Fe]$^-$/RX systems

The reaction between the Fe(II)-containing [Ph$_3$Fe]$^-$ and vinyl iodide behaves somewhat differently than the previous cases. [Ph$_3$Fe]$^-$ is predicted to have a quintet ground state, with the singlet and triplet states being much higher in energy by 123 and 71 kJ mol^{-1}, respectively (Figure S53).[15] Binding of alkene in the π complex is much less strong than that for the [Ph$_2$Fe]$^-$/C$_2$H$_3$I system (by 50 instead of 140 kJ mol^{-1}) due to steric and electronic effects (Figures 4 and S44). The C–I bond activation step still has a fairly modest barrier relative to the complex, but is rather close in energy to the entrance channel (−18 kJ mol^{-1}), which might in part account for the experimentally undetectable reaction efficiency. However, a more important factor concerns the role of spin-state change. The key C–I bond activation TS has a triplet ground state, with all located TSs on the quintet surface being significantly higher in energy. The π complex formed by adding vinyl iodide has near-degenerate quintet and triplet states, which might suggest that spin-state change would be easy.[16] However, these species have quite

Chem. Eur. J. **2022**, *28*, e202202030 (5 of 8)

© 2022 The Authors. Chemistry - A European Journal published by Wiley-VCH GmbH

Chemistry–A European Journal

Research Article
doi.org/10.1002/chem.202202030

Chemistry Europe
European Chemical
Societies Publishing

different coordination geometries around the central iron atom, and different degrees of distortion of the bound vinyl iodide, and this leads to a significant potential energy barrier for spin-state change, with the minimum energy crossing point (MECP)[17] lying 43 kJ mol^{-1} above the quintet minimum. As a result of the quite weak binding of the π complex, this is just 11 kJ mol^{-1} below the reactants (Figure S54). Given the entropic cost of binding and of spin-state change, this suggests that crossing to the triplet surface is not facile, thereby accounting for the lack of reactivity. The hypothetical Fe(III) halogen transfer product Ph$_3$FeI$^-$ is predicted to have a sextet ground state (forming overall quintet or septet states in combination with the radical co-product), with the doublet and quartet states being higher in energy only by 11 and 3 kJ mol^{-1}, respectively (Figures 4 and S53).

In the case of [Ph$_3$Fe]$^-$/C$_3$H$_5$Br, however, slow reaction was observed, leading to cross-coupling. In this case, stabilization of the product allyl radical means that the reaction energy for halogen transfer remains negative at −66 kJ mol^{-1}, and the calculated C–Br activation TS lies lower in energy than reactants (by 20 kJ mol^{-1}, see Figure S55), consistent with some observed reactivity in the experiment. As for the case of reaction with vinyl iodide, the lowest halogen-activation TS lies on the triplet surface, though the lowest-energy quintet TS is not much higher in energy, perhaps because this C–Br activation TS is stabilized by π interaction between the Fe atom of [Ph$_3$Fe]$^-$ and the allyl double bond (Figures S46 and S55). The quintet and triplet forms of the π complex are only moderately strongly bound, by 61 and 44 kJ mol^{-1}, respectively (Figure S55), but

they differ somewhat less in structure than in the case of vinyl iodide, such that the MECP lies lower in energy, 26 kJ mol^{-1} lower than reactants (Figure S54), which together with significant spin-orbit coupling may allow some spin-state change and reaction on the triplet surface. It is also possible that the lower energy of the quintet TS enables some reaction on that surface. After C–Br activation, a low-energy [Ph$_3$Fe(C$_3$H$_5$)Br]$^-$ intermediate is formed that can undergo reductive elimination over a low barrier, yielding ultimately allylbenzene and [Ph$_2$FeBr]$^-$, which in common with related Fe(II) species is predicted to have a quintet ground state (Figure S55).

Conclusion

We have investigated the microscopic reactivity of phenyl-ferrate anions toward organyl halides by a combination of tandem mass spectrometry and DFT calculations. The reactivity of the iron complexes depends strongly on their oxidation state, ligation, and nuclearity. [Ph$_2$Fe(I)]$^-$ and other low-valent ferrates are significantly more reactive than [Ph$_3$Fe(II)]$^-$ whereas [Ph$_4$Fe(III)]$^-$ was found to be inert to all of the probed substrates. The coordination of PPh$_3$ to the metal center and the increase of the nuclearity also lower the reactivity. Moreover, the reaction efficiency varies for different organyl halides RX, with the organyl iodides in most cases being more reactive than the corresponding organyl bromides or chlorides. A first reaction channel operative for both [Ph$_2$Fe(I)]$^-$ and [Ph$_3$Fe(II)]$^-$ does not halt at the stage of the oxidative adduct, but directly
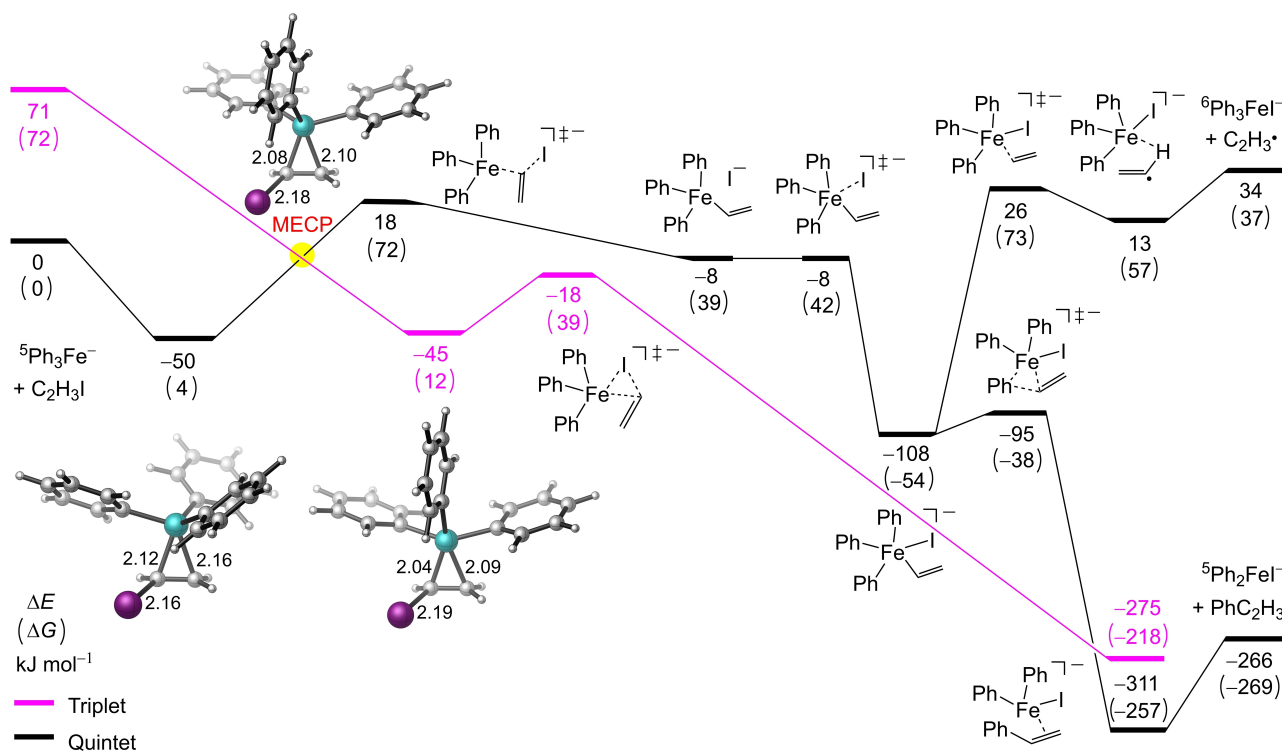
Figure 4. Potential and free energy surface for the [Ph$_3$Fe]$^-$/C$_2$H$_3$I system (for $T = 298.15$ K). Structures of the π complex and the minimum energy crossing point between triplet and quintet are shown, with selected interatomic distances (Å).

Chem. Eur. J. **2022**, *28*, e202202030 (6 of 8)

© 2022 The Authors. Chemistry - A European Journal published by Wiley-VCH GmbH

Chemistry–A European Journal

Research Article
doi.org/10.1002/chem.202202030

**Chemistry
Europe**
European Chemical
Societies Publishing

releases the cross-coupling product. Our DFT calculations suggest that the reactions starting from $[Ph_2Fe(I)]^-$ involve considerably lower barriers than those starting from $Ph_3Fe(II)^-$, thus explaining the higher reaction rates observed for the former. While the reaction of $[Ph_2Fe(I)]^-$ proceeds entirely on the quartet surface, that of its $[Ph_3Fe(II)]^-$ counterpart requires a spin change from the quintet to the triplet state. This spin change imposes an additional constraint and contributes to the lowered reactivity of $[Ph_3Fe(II)]^-$ observed in the experiments.

Besides undergoing direct cross-coupling, the $[Ph_2Fe(I)]^-$ complex also abstracts a halogen atom from most of the probed substrates to afford free organyl radicals. This pathway highlights the propensity of organoiron species toward radical reactions. In solution, such halogen-transfer reactions could afford unwanted byproducts or, alternatively, also furnish the desired cross-coupling products by a radical-rebound mechanism followed by a reductive elimination. Although the present gas-phase study, thus, obviously does not include all aspects of the full catalytic system in solution, the obtained insight into the intrinsic reactivity of the phenylferrate complexes helps to improve our mechanistic understanding of iron-catalyzed cross-coupling reactions. Together with further investigations, it thereby also promises to assist in the systematic and rational development and optimization of these transformations.

Experimental and Theoretical Section

Experimental methods: Solutions of $Fe(acac)_3$ (acac = acetylacetonato, 20 mm, 1.0 eq), $PhMgCl$ (4.0 eq), and PPh_3 (2.0 eq) in dry THF (freshly distilled from sodium/benzophenone) were injected into the electrospray ionization (ESI) source of an HCT quadrupole-ion trap mass spectrometer (Bruker Daltonik) at a flow rate of 8 $\mu L\,min^{-1}$. The ESI source was operated with an ESI voltage of 3000 V and nitrogen as dry (0.7 bar backing pressure, 333 K) and nebulizer gas (5–10 $mL\,min^{-1}$) to afford a series of phenylferrate anions. After mass selection with typical isolation widths of 4.0 u, the phenylferrate anions were directly investigated or first subjected to energetic collisions with helium gas ($p \approx 6 \times 10^{-4}$ mbar) to produce further phenylferrates by means of fragmentation reactions (Scheme S1).

For probing the bimolecular reactivity of the phenylferrates at $T \approx 300$ K,[18,19] the mass-selected ions of interest were allowed to react with the substrate RX in the ion trap for given times t. The substrate, together with the helium, was constantly introduced into the ion trap from a reservoir, into which a defined quantity of the former had been added via a μL-syringe and freed from traces of air by a freeze-pump cycle.[19] Filling-up of the reservoir with helium gas to a pressure of 6.0 bar resulted in a well-defined He/RX ratio in the reservoir, which permitted the calculation of the partial pressure $p(RX)$ in the ion trap from the known total pressure in the ion trap and the relative diffusion constants of He and RX.[18b,20] The measured normalized signal intensities of residual reactant ions and newly formed product ions as functions of the reaction time were then analyzed with the GEPASI program[21] to determine bimolecular rate constants k_2. From these rate constants and collision rates k_{coll} estimated by capture theory,[22] reaction efficiencies $\phi = k_2/k_{coll}$ were calculated (Table S1, Supporting Information).

Theoretical methods: All DFT calculations were carried out using Gaussian 16 (Revision A.03).[23] Geometry optimizations were performed applying the B3LYP[24] functional including dispersion

correction D3BJ,[25] using the all-electron def2SVP[26] basis sets for Fe, C and H, and the combination of the SDD[27] effective core potential and the def2SVP valence basis set for I and Br. Frequency calculations were performed at the same level of theory and used to obtain Gibbs energy corrections at 298.15 K. Refined single point energies were obtained for the optimized geometries at the B3LYP-D3BJ/def2TZVP level of theory which together with the zero-point corrections obtained with the smaller basis set are the basis for the relative energies reported in the text. MECP structures were optimized with Gaussian 16 together with an in-house script[17] based on energies and gradients on the two potential energy surfaces computed with B3LYP-D3BJ/def2SVP as above, and their energies refined using large-basis set single point calculations. Their relative energies are given based on electronic energies only. Intrinsic reaction coordinate computations were performed to verify connectivity of the TSs and minima. Benchmarking CCSD(T)-F12[28] calculations were performed with the Molpro software,[29] the aug-cc-pwCVTZ basis set for Fe and the cc-pVDZ-F12 basis set for C and H. Further details on all these aspects are provided in the Supporting Information.

Conflict of Interest

The authors declare no conflict of interest.

Data Availability Statement

The data that support the findings of this study are available in the supplementary material of this article.

[1] a) M. Tamura, J. Kochi, J. Am, Chem. Soc. Rev. **1971**, 93, 1487–1489; b) H. Avedissian, G. Cahiez, Synthesis **1998**, 8, 1199–1205; c) A. Fürstner, A. Leitner, M. Mendez, H. Krause, J. Am, Chem. Soc. Rev. **2002**, 124, 13856–13863; d) R. Martin, A. Fürstner, Angew. Chem. **2004**, 116, 4045–4047; Angew. Chem. Int. Ed. **2004**, 43, 3955–3957; e) T. Hatakeyama, M. Nakamura, J. Am, Chem. Soc. Rev. **2007**, 129, 9844–9845; f) G. Cahiez, V. Habiak, C. Duplais, A. Moyeux, Angew. Chem. **2007**, 119, 4442–4444; Angew. Chem. Int. Ed. **2007**, 46, 4364–4366; g) T. Hatakeyama, S. Hashimoto, K. Ishizuka, M. Nakamura, J. Am, Chem. Soc. Rev. **2009**, 131, 11949–11963; h) W. M. Czaplik, M. Mayer, A. Jacobi von Wangelin, Angew. Chem. **2009**, 121, 616–620; Angew. Chem. Int. Ed. **2009**, 48, 607–610; i) A. K. Steib, T. Thaler, K. Komeyama, P. Mayer, P. Knochel, Angew. Chem. **2011**, 123, 3361–3365; Angew. Chem. Int. Ed. **2011**, 50, 3303–3307; j) S. Gülak, A. Jacobi von Wangelin, Angew. Chem. **2012**, 124, 1386–1390; Angew. Chem. Int. Ed. **2012**, 51, 1357–1361; k) M. Jin, L. Adak, M. Nakamura, J. Am, Chem. Soc. Rev. **2015**, 137, 7128–7134; l) O. M. Kuzmina, A. K. Steib, A. Moyeux, G. Cahiez, P. Knochel, Synthesis

2015, *47*, 1695–1705; m) R. Greiner, R. Blanc, C. Petermayer, K. Karaghiosoff, P. Knochel, *Synlett* **2016**, *27*, 231–236.

[2] a) J. A. Przyojski, K. P. Veggeberg, H. D. Arman, Z. J. Tonzetich, *ACS Catal.* **2015**, *5*, 5938–5946; b) T. Parchomyk, K. Koszinowski, *Synthesis* **2017**, *49*, 3269–3280; c) N. J. Bakas, M. L. Neidig, *ACS Catal.* **2021**, *11*, 8493–8503.

[3] a) A. Fürstner, R. Martin, H. Krause, G. Seidel, R. Goddard, C. W. Lehmann, *J. Am. Chem. Soc.* **2008**, *130*, 8773–8787; b) A. Hedström, U. Bollmann, J. Bravidor, P.-O. Norrby, *Chem. Eur. J.* **2011**, *17*, 11991–11993; c) R. B. Bedford, *Acc. Chem. Res.* **2015**, *48*, 1485–1493; d) S. L. Daifuku, J. L. Kneebone, B. E. R. Snyder, M. L. Neidig, *J. Am. Chem. Soc.* **2015**, *137*, 11432–11444; e) M. Clémancey, T. Cantat, G. Blondin, J.-M. Latour, P. Dorlet, G. Lefèvre, *Inorg. Chem.* **2017**, *56*, 3834–3848.

[4] a) K. Vikse, T. Naka, J. S. McIndoe, M. Besora, F. Maseras, *ChemCatChem* **2013**, *5*, 3604–3609; b) K. Vikse, G. N. Khairallah, A. Ariafard, A. J. Canty, R. A. J. O'Hair, *J. Am. Chem. Soc.* **2015**, *137*, 13588–13593; c) S. Muramatsu, K. Koyasu, T. Tsukuda, *J. Phys. Chem. A* **2016**, *120*, 957–963; d) K. Greis, Y. Yang, A. J. Canty, R. A. J. O'Hair, *J. Am. Soc. Mass Spectrom.* **2019**, *30*, 1867–1880.

[5] a) R. B. Bedford, P. B. Brenner, E. Carter, P. M. Cogswell, M. F. Haddow, J. N. Harvey, D. M. Murphy, J. Nunn, C. H. Woodall, *Angew. Chem.* **2014**, *126*, 1835–1839; *Angew. Chem. Int. Ed.* **2014**, *53*, 1804–1808; b) C.-L. Sun, H. Krause, A. Fürstner, *Adv. Synth. Catal.* **2014**, *356*, 1281–1291; c) M. H. Al-Afyouni, K. L. Fillman, W. W. Brennessel, M. L. Neidig, *J. Am. Chem. Soc.* **2014**, *136*, 15457–15460; d) S. B. Muñoz III, S. L. Daifuku, W. W. Brennessel, M. L. Neidig, *J. Am. Chem. Soc.* **2016**, *138*, 7492–7495; e) F. E. Zhurkin, M. D. Wodrich, X. A. Hu, *Organometallics* **2017**, *36*, 499–501; f) J. D. Sears, S. B. Muñoz III, M. C. Aguilera Cuenca, W. W. Brennessel, M. L. Neidig, *Polyhedron* **2019**, *158*, 91–96; g) J. D. Sears, S. B. Muñoz III, S. L. Daifuku, A. A. Shaps, S. H. Carpenter, W. W. Brennessel, M. L. Neidig, *Angew. Chem.* **2019**, *131*, 2795–2799; *Angew. Chem. Int. Ed.* **2019**, *58*, 2769–2773; h) L. Rousseau, C. Herrero, M. Clémancey, A. Imberdis, G. Blondin, G. Lefèvre, *Chem. Eur. J.* **2020**, *26*, 2417–2428; i) L. Rousseau, N. Touati, L. Binet, P. Thuéry, G. Lefèvre, *Inorg. Chem.* **2021**, *60*, 7991–7997; j) E. Zhou, P. Chourreu, N. Lefèvre, M. Ahr, L. Rousseau, C. Herrero, E. Gayon, G. Cahiez, G. Lefèvre, *ACS Org. Inorg. Au*, in press, doi: . 10.1021/acsorginorgau.2c00002.

[6] a) T. Parchomyk, K. Koszinowski, *Chem. Eur. J.* **2016**, *22*, 15609–15613; b) T. Parchomyk, S. Demeshko, F. Meyer, K. Koszinowski, *J. Am. Chem. Soc.* **2018**, *140*, 9709–9720.

[7] P. Chen, *Angew. Chem.* **2003**, *115*, 2938–2954; *Angew. Chem. Int. Ed.* **2003**, *42*, 2832–2847.

[8] R. A. J. O'Hair, *Chem. Commun.* **2006**, *42*, 1469–1481.

[9] K. L. Vikse, J. S. McIndoe, *Pure Appl. Chem.* **2015**, *87*, 361–377.

[10] D. Agrawal, E.-L. Zins, D. Schröder, *Chem. Asian J.* **2010**, *5*, 1667–1676.

[11] a) P. Lahuerta, J. Payá, X. Solans, M. A. Ubeda, *Inorg. Chem.* **1992**, *31*, 385–391; b) A. Boddien, F. Gärtner, R. Jackstell, H. Junge, A. Spannenberg, W. Baumann, R. Ludwig, M. Beller, *Angew. Chem.* **2010**, *122*, 9177–9181; *Angew. Chem. Int. Ed.* **2010**, *49*, 8993–8996; c) D. Wang, M. Li, C. Shuang, Y. Liang, Y. Zhao, M. Wang, Z. Shi, *Nat. Commun.* **2022**, *13*, 2394.

[12] J. Hioe, H. Zipse, in *Encyclopedida of Radicals in Chemistry, Biology and Materials*, Wiley, **2012**.

[13] For similar dynamical effects, see J. A. Nummela, B. K. Carpenter, *J. Am. Chem. Soc.* **2002**, *124*, 8512–8513, addition/correction: ibid **2002**, 124, 14810, and refs. therein.

[14] The comparison of energy barriers for estimating relative reaction efficiencies is only valid for reactions of a similar type (such as reductive eliminations), but not for those of different types (such as homolysis and reductive eliminations) because the latter will strongly differ in their entropic characteristics.

[15] Previous calculations also found a quintet ground state for this ion, but with a smaller spin-state gap, see ref. 4 h. Presumably, this smaller spin-state gap results from the use of a GGA functional. Our CCSD(T) benchmark supports the accuracy of B3LYP-D3 for this system (see Table S2).

[16] J. N. Harvey, *WIREs Comput. Mol. Sci.* **2014**, *4*, 1–14.

[17] J. N. Harvey, M. Aschi, H. Schwarz, W. Koch, *Theor. Chem. Acc.* **1998**, *99*, 95–99.

[18] a) S. Gronert, *J. Am. Soc. Mass Spectrom.* **1998**, *9*, 845–848; b) T. Waters, R. A. J. O'Hair, A. G. Wedd, *J. Am. Chem. Soc.* **2003**, *125*, 3384–3396.

[19] T. Parchomyk, K. Koszinowski, *J. Mass Spectrom.* **2019**, *54*, 81–87.

[20] S. Gronert, L. M. Pratt, S. Mogali, *J. Am. Chem. Soc.* **2001**, *123*, 3081–3091.

[21] a) P. Mendes, *Bioinformatics* **1993**, *9*, 563–571; b) P. Mendes, *Trends Biochem. Sci.* **1997**, *22*, 361–363; c) P. Mendes, D. B. Kell, *Bioinformatics* **1998**, *14*, 869–883.

[22] a) W. J. Chesnavich, T. Su, M. T. Bowers, *J. Chem. Phys.* **1980**, *72*, 2641–2655; b) K. F. Lim, *Quantum Chem. Program Exch. Bull.* **1994**, *14*, 3.

[23] Gaussian 16, Revision A.03, M. J. Frisch, G. W. Trucks, H. B. Schlegel, G. E. Scuseria, M. A. Robb, J. R. Cheeseman, G. Scalmani, V. Barone, G. A. Petersson, H. Nakatsuji, X. Li, M. Caricato, A. V. Marenich, J. Bloino, B. G. Janesko, R. Gomperts, B. Mennucci, H. P. Hratchian, J. V. Ortiz, A. F. Izmaylov, J. L. Sonnenberg, D. Williams-Young, F. Ding, F. Lipparini, F. Egidi, J. Goings, B. Peng, A. Petrone, T. Henderson, D. Ranasinghe, V. G. Zakrzewski, J. Gao, N. Rega, G. Zheng, W. Liang, M. Hada, M. Ehara, K. Toyota, R. Fukuda, J. Hasegawa, M. Ishida, T. Nakajima, Y. Honda, O. Kitao, H. Nakai, T. Vreven, K. Throssell, J. A. Montgomery Jr., J. E. Peralta, F. Ogliaro, M. J. Bearpark, J. J. Heyd, E. N. Brothers, K. N. Kudin, V. N. Staroverov, T. A. Keith, R. Kobayashi, J. Normand, K. Raghavachari, A. P. Rendell, J. C. Burant, S. S. Iyengar, J. Tomasi, M. Cossi, J. M. Millam, M. Klene, C. Adamo, R. Cammi, J. W. Ochterski, R. L. Martin, K. Morokuma, O. Farkas, J. B. Foresman, D. J. Fox, Gaussian, Inc., Wallingford CT, **2016**.

[24] A. D. Becke, *J. Chem. Phys.* **1993**, *98*, 5648–5652.

[25] S. Grimme, S. Ehrlich, L. Goerigk, *J. Comput. Chem.* **2011**, *32*, 1456–1465.

[26] F. Weigend, R. Ahlrichs, *Phys. Chem. Chem. Phys.* **2005**, *7*, 3297–3305.

[27] A. Bergner, M. Dolg, W. Küchle, H. Stoll, H. Preuß, *Mol. Phys.* **1993**, *80*, 1431–1441.

[28] a) T. B. Adler, G. Knizia, H.-J. Werner, *J. Chem. Phys.* **2007**, *127*, 221106; b) H.-J. Werner, G. Knizia, F. R. Manby, *Mol. Phys.* **2011**, *109*, 407–417.

[29] a) H.-J. Werner, P. J. Knowles, G. Knizia, F. R. Manby, M. Schütz, *WIREs Comput. Mol. Sci.* **2012**, *2*, 242–253; b) H.-J. Werner, P. J. Knowles, G. Knizia, F. R. Manby, M. Schütz, et al., MOLPRO, version 2015.1, a package of ab initio programs, see http://www.molpro.net.